

Spontaneous magnetization and domain formation in ferromagnets near the Curie point

G. M. Drabkin, E. I. Zabidarov, and A. V. Kovalev

Leningrad Institute of Nuclear Physics, USSR Academy of Sciences
(Submitted May 26, 1976)
Zh. Eksp. Teor. Fiz. 69, 1804–1816 (November 1975)

A region of quasi-homogeneous magnetization in ferromagnets near the temperature of the second-order phase transition in a zero external field is observed by the polarized-neutron technique. The domain formation temperature T_d is determined from the change of the spectral dependence of the depolarization of neutrons traversing the sample with temperature and from the maximal value of the derivative of the polarization with respect to temperature $\partial P/\partial T$ on the $P(T)$ curve. The Curie point T_c is found on the basis of the appearance of a magnetic moment in the sample. The value of T_d is about $0.1\text{--}3^\circ$ below T_c , depending on the type of the magnetic substance. The quasi-homogeneous magnetization region exists in the $T_d < T \leq T_c$ temperature range.

PACS numbers: 75.25.+z, 75.30.Jy

It is known that critical fluctuations of the magnetization take place in ferromagnets near the phase-transition temperature T_c . These are regions of correlated atomic spins, the dimensions and magnetizations of which depend on the proximity to the Curie point T_c , i.e., on the quantity $\tau = |T - T_c|/T_c$. With increasing temperature, however, at $T > T_c$, the fluctuations vanish and the sample goes over into the ordinary paramagnetic state. At $T < T_c$, with decreasing temperature, domains are produced in the sample after the onset of the spontaneous magnetization. The domain structure of the ferromagnets is due to the presence of magnetic or dipole-dipole forces and is determined mainly by the magnetization, anisotropy, and geometry of the sample.

The available data^[1,2] indicate that domains exist also in the immediate vicinity of the Curie point. Despite the fact that the magnitude of the spontaneous magnetization changes strongly as $T \rightarrow T_c$, the domain structure in the sample depends little on the temperature. It is particularly difficult to investigate the critical region $\tau \sim 10^{-3}\text{--}10^{-5}$, where the processes of greatest interest for the study of phase transitions take place. The equilibrium thermodynamic properties of magnets near T_c are expressed in the form of functions of τ . The question of the exact determination of the Curie temperature is therefore of fundamental significance. Yet the known experimental methods of determining T_c have significant shortcomings.

The classical magnetic methods of determining the Curie point are not accurate enough and as a rule depend on the method of extrapolating the quantities measured in a finite magnetic field to a zero external field. In those methods where T_c is determined from the singularities of the behavior of the thermodynamic properties of the magnet,^[3] the anomalies of these properties can appear more strongly at the domain-formation temperature than at T_c . If T_c and T_d are close, these methods are unable to reveal the singularities of the phase transition at the Curie point itself. In addition the external magnetic field influences the nature of the phase transition. The method of polarized neutrons is free of the foregoing shortcomings.

This paper is devoted to a study of phenomena near a second-order phase transition. We investigated the onset of an ordered magnetic state in ferromagnets, and domain formation in a sample in a zero external field.

We have used for this purpose the latest advances in the polarized-neutron procedure.

EXPERIMENT

The polarized-neutron method consists of studying the behavior of the polarization vector of the neutrons passing through the ferromagnet, as a function of the sample temperature. The passage of a beam of polarized neutrons through ferromagnetic media has been sufficiently well studied theoretically. In the experiment it is necessary to distinguish between the processes of rotation of the polarization and the decrease of its length, i.e., depolarization. For an experimental observation of the state of magnetization of the sample, two essentially new devices were added to the previously developed polarized-neutron setup: 1) a device for the analysis of all three projections of the polarization vector; 2) monochromators for a simultaneous measurement of the polarization of the neutrons with different wavelengths.

The general arrangement of the setup and the tasks of its main units are shown in Fig. 1. Thermal-spectrum polarized with wavelengths $\lambda \geq \lambda_{ep}$ (λ_{ep} is the end-point wavelength in the neutron spectrum and corresponds to the critical angle of reflection from the mirror) were obtained by reflection from a magnetic mirror.

The polarizer and analyzer mirrors were 440 mm long. They were prepared by evaporating a CoFe (50%) alloy on polished glass, with an intermediate sublayer of a titanium-gadolinium alloy. The thickness of the Ti + Gd sublayer was $\sim 1 \mu$, thus ensuring total absorption of the neutrons not reflected from the CoFe ferromagnetic film. These mirrors made it possible to obtain a polarized beam of neutrons ($\lambda \sim 4 \text{ \AA}$) with polarization $P_0 \approx 96\%$.

1. Analysis of the Projections of the Neutron-Beam Polarization Vector

The unit for the measurement of the polarization-vector projections operates on the principle of nonadiabatic introduction of the neutron spin into a system of mutually-perpendicular magnetic fields directed along the coordinate axes. The non-adiabaticity condition $K = \omega_L/\omega_0 \ll 1$ at $K = 0.1$ is satisfied with 1% accuracy. Here $\omega_L = gH$ is the spin Larmor-precession frequency

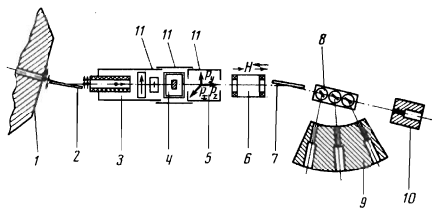


FIG. 1. Setup with polarized neutrons for the study of phase transitions in ferromagnets: 1—reactor, 2—polarizing mirror, 3—system of solenoids for the orientation of the polarization vector at the entrance in the sample, 4—thermostat with sample, 5—setup for the measurement of the polarization-vector projections, 6—neutron spin flipper, 7—analyzing mirror, 8—monochromator crystals, 9—monochromatic-beam detectors, 10—detector for the mirror beam remaining after the monochromator, 11—magnetic screens.

in the field H , g is the neutron gyromagnetic ratio, and ω_0 is the frequency of rotation of the magnetic field in terms of the coordinates of the moving neutrons. The method for the coordinates of the projections was developed by Okorokov and co-workers in our laboratory.^[5,6] One of the variants of the analyzing apparatus was used in the setup and its diagram is shown in Fig. 2. The field of the solenoid H_z was turned on for the measurement of the projection P_z , and the field of the magnet H was additionally turned on to measure the two other projections P_x and P_y . The field in the magnet was set in succession along the axes x and y by rotating the magnet about its own axis z . The projections were measured with 3% accuracy. The entire setup together with the sample were carefully screened against the magnetic fields of the apparatus. The direction of the incident-neutron polarization vector was set with the aid of an analogous arrangement. Measurement of the three components of the polarization vector makes it possible to distinguish between rotation and depolarization and to measure in some cases the magnetization of the sample.

2. Spectral Analysis of Neutron Polarization

The setup with ferromagnetic mirrors produce a continuous spectrum of polarized neutrons. To separate monochromatic lines from the spectrum, three monochromator crystals of pyrolytic graphite were placed in the neutron path in tandem past the analyzer mirror. The neutrons reflected from each crystal entered a separate detector and the produced pulses were registered by a multichannel setup. Using the different spectral dependence of the neutron depolarization, one can determine the magnetic structure of the sample, the dimensions of the magnetic inhomogeneities, and the values of their magnetization.

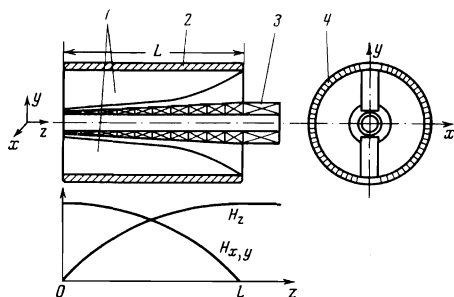


FIG. 2. Diagram of setup for the measurements of the projections of the polarization vector and magnetic-field configuration in the setup: 1—pole pieces, 2—yoke of electromagnet, 3—variable-cross-section solenoid with field $H_z = H_0 \sin(\pi z/2L)$, 4—electromagnet winding; $H_{x,y} = H_0 \cos(\pi z/2L)$.

We used in the present study simultaneously three neutron wavelengths: $\lambda_1 = 3.20 \pm 0.06 \text{ \AA}$, $\lambda_2 = 4.00 \pm 0.08 \text{ \AA}$, and $\lambda_3 = 4.8 \pm 0.1 \text{ \AA}$.

The investigated samples were placed in a vacuum oven that contained no magnetic materials. The external magnetic field at the sample location was less than 0.01 Oe, and the temperature was maintained stable during the measurements within 0.01°C.

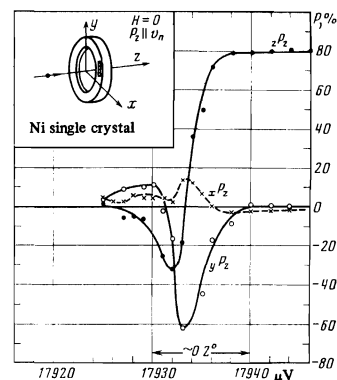
3. Measurement Results

The first measurement object was a nickel sample, cut from a single crystal, in the form of a ring 6 mm thick and with inside and outside diameters 15 and 22 mm.

Figure 3 shows the geometry of the experiment and the temperature dependence of the components P_z of the polarization vector of the neutrons passing through the sample, whereas the polarization vector of the incident neutrons was oriented in succession along the three directions x (xP_0), y (yP_0), and z (zP_0). The plane of the ring coincided with a crystallographic plane of the (100) type. It is known that the easy magnetization direction [111] in the Ni crystal makes angles 55° with the [100] directions. The polarization vector of the neutrons incident on the target was approximately oriented along directions of the [100] type and consequently made a rather large angle, close to $\pi/2$, with the easy-magnetization axis. It follows from the foregoing data that when the sample temperature is lowered a spontaneous magnetization is produced in the sample and causes rotation of the polarization vector. The instant when magnetization appears in the sample is particularly clearly revealed by the rotation of the vector yP_0 towards the z axis and by the subsequent appreciable growth of its projection yP_z in the temperature interval $\Delta T \sim 0.15^\circ\text{C}$ as a result of the rotation. With further decrease of temperature, the principal role in the change of the polarization vectors is assumed by depolarization. The depolarization process becomes possible when a random domain structure is produced in the sample. It is obvious that in this experiment the behavior of the polarization vector was strongly influenced by the closed shape of the sample and by the mutual orientation of the directions of the easy magnetization and the polarization vectors.

The results of the experiment show that when T_c is approached from the high-temperature side the spontaneous magnetization in the sample is observed before any noticeable depolarization zP_z is revealed. The critical fluctuations near T_c depolarize the beam weakly. The reason is that the effective magnetization

FIG. 3. Dependence of the projection of the polarization vector P_z on the temperature for neutrons with $\lambda = 4 \text{ \AA}$, passing through an annular Ni single crystal. The vector of the polarization ahead of the sample was oriented in succession along the coordinate axes x , y , and z . The abscissas in this and succeeding figures represent the temperature as measured with a copper-constantan thermocouple (the thermoelectric power).



of the fluctuations, which acts on the neutron spin, is small on account of the rapidly decreasing distribution of the magnetization within the limits of the fluctuations. According to the estimates of Maleev and Ruban,^[7] the critical depolarization of the neutrons is $\Delta P \lesssim 1\%$.

The results of a second variant of an experiment with nickel are shown in Fig. 4. In this case the polarization vector was oriented arbitrarily prior to passing through the sample, and its three projections P_x , P_y , and P_z were measured after emerging from the sample. The sample was likewise in a zero magnetic field ($H < 0.01$ Oe, and the neutron wavelength was $\lambda = 2.78 \text{ \AA}$. The projections of the polarization vector of the incident neutrons correspond to the values indicated in Fig. 4 at a temperature $T \gg T_C$. The onset of magnetization in the sample is revealed by the increase of the projection P_y . The behavior of all the projections of the polarization vector, particularly the large negative value of P_x , offer evidence of rotation of the polarization vector through large angles ($\sim \pi/2$), and by the same token of the existence in the sample of magnetization regions with dimensions of several millimeters, of the type of magnetization modes. Figure 4 shows also the variation of the absolute magnitude of the polarization vector with temperature. It is seen from these relations that the abrupt depolarization and the large changes in the values of the polarization-vector projections occur at a lower temperature than the onset of the magnetization.

The rotation of the polarization vector is thus observed in these experiments at a temperature higher than the appreciable depolarization of the beam.

In the second series of analogous experiments we obtained the results obtained in Fig. 5 for a uniaxial ferrimagnet—hexagonal barium ferrite ($\text{BaFe}_{12}\text{O}_{19}$). The Curie point of this ferrite is $T_C = 723^\circ\text{K}$, and the direction of the easy magnetization coincides with the hexagonal c axis. At room temperature the saturation magnetization is $4\pi M = 4775 \text{ G}$, and the anisotropy field is $H_A \approx 17 \text{ kOe}$.^[8] We used a single-crystal ferrite measuring $5 \times 6 \times 4 \text{ mm}$. We measured the polarization of the transmitted beam as a function of the temperature for two directions of the polarization vector of the incident neutrons. The geometry of the experiment is shown likewise in Fig. 5. In the first case, the polarization vector ahead of the sample, zP_0 , coincided within several per cent with the anisotropy axis of the sample, which was directed along the coordinate axis z , and we measured its projection zP_z on the z axis after passing through the sample. In the second case the polariza-

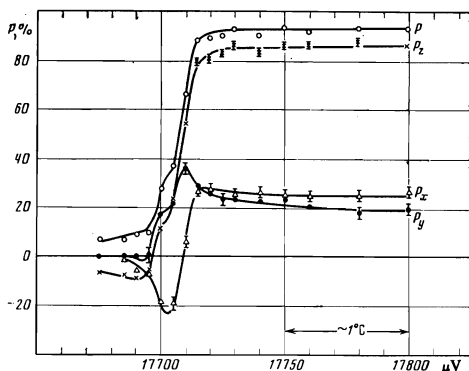


FIG. 4. Temperature dependence of the projections and of the absolute magnitude of the polarization vector for neutrons with $\lambda = 2.78 \text{ \AA}$ after passing through an annular Ni single crystal.

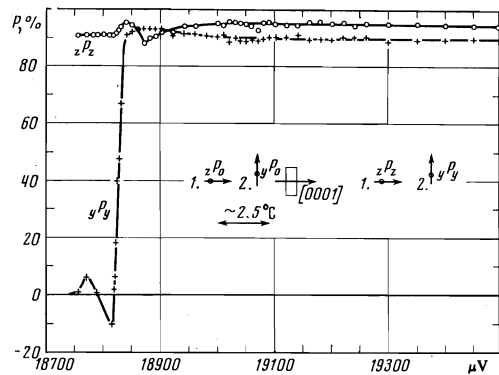


FIG. 5. Temperature dependences of the projections yP_y and zP_z after passage of neutrons with $\lambda = 2.78 \text{ \AA}$ through a barium hexaferrite single crystal.

tion vector yP_0 of the incident neutrons was perpendicular to the c axis and we measured its projection yP_y . In the phase-transition region, the projection yP_y drops abruptly to zero, and zP_z decreases by only 5% and retains its value up to room temperature. This means that the spontaneous magnetization in the sample becomes aligned along the c axis. The small value of the depolarization of zP_z in the region $T < T_C$ can be attributed to irregularities in the magnetic structure and to depolarization on the domain walls. The rise (3%) in the value of yP_y prior to the abrupt fall-off and the dip in zP_x are obviously connected with the fact that the vectors zP_0 and yP_0 are not exactly aligned with the axes z and y . The spontaneous magnetization produced in the sample by rotating the polarization vector changes the projections of these vectors in the manner indicated above.

Thus, we have observed in this experiment the onset of spontaneous magnetization in a sample at a temperature higher than that corresponding to the start of a substantial depolarization of the neutrons.

The subsequent measurements were made on a polycrystalline yttrium iron garnet (YIG). It is of interest to compare the determination of T_C by the magnetic method with experiments on depolarization. Figures 6 and 7 show the results of a simultaneous measurement, on one sample, of the magnetic moment induced by the external field, and of the depolarization of neutrons of three wavelengths as functions of the temperature at $H = 0$. It is seen from the figures that the maximum of $\partial P/\partial T$ corresponds approximately to the point where the $M(T)$ curve has a kink as $H \rightarrow 0$. In the same temperature region one observes a change in the spectral dependence of the neutron depolarization, due to the corresponding realignment of the magnetic structure of the sample. In the lower part of Fig. 7 is shown the temperature dependence of the exponent n in the equation $\ln(P/P_0) \sim \lambda^n$ for the depolarization as a function of the neutron wavelength. This question will be discussed in greater detail later on.

Figure 8 shows the results of a simultaneous measurement of the temperature dependences of the depolarization of the transmitted beam and of the intensity of the neutrons scattered through an angle $\theta = 10'$, for single-crystal nickel. The neutrons scattered by the sample through an angle $\theta = 10'$ were passed through the analyzer mirror and registered by a separate detector. The polarization of the transmitted neutrons was analyzed by an analyzer mirror. These neutrons

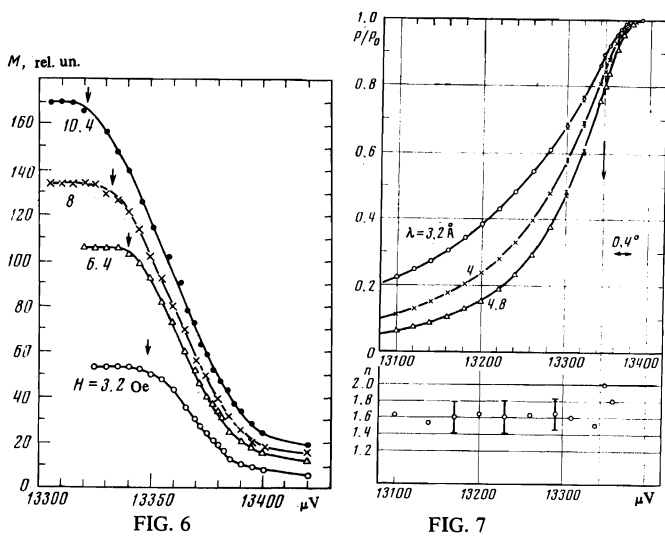


FIG. 6. Temperature dependence of the magnetic moment M of the iron-yttrium iron garnet near the phase transition. The numbers on the curves indicate the values of the external field H (in Oe). The arrows indicate the temperature $T_t(H)$ at which the $M(T)$ curve has a kink.

FIG. 7. Temperature dependence of the depolarization of neutrons with various wavelengths for an iron-yttrium iron garnet in a field $H = 0$, and values of the exponent n in the formula $\ln(P/P_0) \sim \lambda^n$. The value of n was determined accurate to 10%. The arrow indicates the temperature at which pP/p_0 has a maximum.

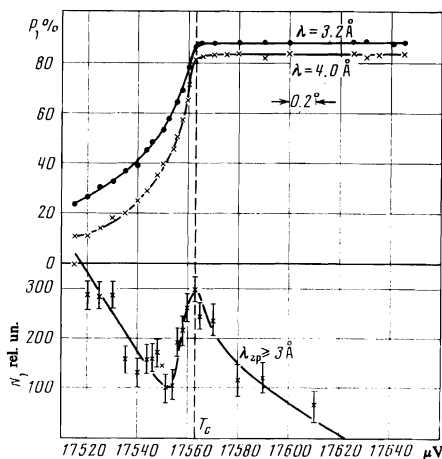


FIG. 8. Temperature dependence of the depolarization of the neutrons (of wavelength λ) in single-crystal Ni, and scattering intensity N of neutrons with $\lambda_{ep} \geq 3 \text{ \AA}$ through an angle $\theta = 10'$ in the absence of an external field.

were then reflected from the monochromator crystals and registered by detectors. The observed peak of the scattered neutrons coincides in temperature with the start of the depolarization.

DISCUSSION OF RESULTS

The Curie point corresponds to the temperature at which spontaneous magnetization sets in the sample. Therefore the start of the rotation of the polarization vector about the spontaneous magnetization, which was observed in our experiment, must indeed be taken to be the Curie point. Estimates show that with the aid of polarized neutrons with $\lambda \approx 5 \text{ \AA}$ it is possible to observe a magnetization on the order of 0.1 G. It is important that such a magnetization was observed in a sample situated in a zero magnetic field.

From the results of measurements on nickel (Figs. 3 and 4) and barium hexaferrite (Fig. 5) we can single out a temperature region in which an abrupt change of polarization takes place. This change is connected with the rotation of the polarization vector and the subsequent decrease of its length on account of the depolarization. As the temperature is lowered, the role of the depolarization process increases, and consequently the polarization of the neutron beam decreases in final analysis to zero. Thus, as T_c is approached from the paramagnetic region, a state close to homogeneous magnetization is produced in the sample and causes large-angle rotation of the polarization vector. This is followed by the breakup of the quasihomogeneous magnetization into regions with dimensions comparable with the sample dimensions. The number of such regions in this temperature interval should be small. The orientation of the magnetization in the regions and the dimensions of these regions are such that the sample has a resultant magnetic moment in some direction. We observe here both rotation of the polarization vector, owing to the presence of an effective moment of the structure, and a depolarization of the beam in individual regions and at their boundaries. With further decrease of the temperature, the dimensions of the regions of spontaneous magnetization decrease, and domains with Bloch walls are produced in the sample. Such a state of the sample causes depolarization of the neutron beam to a zero value.

The described process is accompanied by a continuous growth of the spontaneous magnetization as the temperature is lowered. Inasmuch as the intensity of the critical fluctuations of the magnetization decreases with increasing distance from T_c , the neutron depolarization observed after the onset of the magnetization must be ascribed to the development of the domain-formation process. The temperature interval ΔT from the instant of the onset of spontaneous magnetization to the start of domain formation is different for different substances and depends both on the kind of magnet and apparently also on the value of the saturation magnetization. It follows from Fig. 3 that for nickel the value is $\Delta T \approx 0.1^\circ$ and for the barium ferrite $\Delta T \approx 3^\circ$ (Fig. 5). The dependence of ΔT on the saturation magnetization was observed earlier^[9] for PdFe alloys with different iron-atom concentrations.

On Fig. 5, in the case of uniaxial barium ferrite, it is possible to determine from the behavior of the projection zP_z the temperature at which a domain structure is formed in the sample. This temperature corresponds to the flattening of the plot of the projection zP_z , which remains subsequently constant up to room temperatures. According to powder-pattern investigations, the domain magnetization of hexagonal ferrites (magnetoplumbites)^[10,11] has a preferred direction along the anisotropy axis [001]. In such a structure we can have a resonant behavior of the polarization vector in the case when $\mathbf{P} \perp \mathbf{M}$,^[12] or rotation of \mathbf{P} about the effective moment of the structure. These conclusions are confirmed by the behavior of the polarization vectors shown in Fig. 5.

In the case of polycrystalline samples having an isotropic magnetic structure, the polarized-neutron procedure is inapplicable in practice in its most sensitive part that is connected with large-angle rotation of the polarization vector about the macroscopic magnetic moment of the sample. In this case, the main observa-

ble process is depolarization on the domain structure of the sample. This process was considered theoretically by Halpern and Holstein^[13]. In the case of randomly oriented domains, the neutron depolarization is determined in terms of the average rotation angle of the polarization vector in one domain, $\alpha = \langle \alpha_1 \rangle = gB\tau$:

$$\frac{P}{P_0} = \left[\frac{1+2\langle \cos \alpha \rangle}{3} \right]^N, \quad (1)$$

where $N = L/\delta$ is the number of domains in the path of the neutron beam, L is the thickness of the sample, δ is the average dimension of the domain, $\tau = \delta/v$ is the time of flight of the neutron through one domain, v is the neutron velocity, and B is the average induction in the domain. It was assumed here^[13] that the induction field $B = 4\pi M$ acting on the neutron is homogeneous, and the demagnetization field was disregarded. As shown by Maleev and Ruban,^[7] allowance for the latter leads to a dependence of the magnitude of the depolarization on the orientation of the vector P_0 relative to the neutron-velocity vector v . For small domains, when $\alpha_1 \ll 1$, we obtain from (1) the well known formula

$$\frac{P}{P_0} = \exp \left\{ -\frac{1}{3} g^2 B^2 \frac{\delta L}{v^2} \right\}, \quad (2)$$

and at $\alpha \gtrsim 1$, when $\langle \cos \alpha \rangle = 0$, another relation holds:

$$P/P_0 = (1/3)^{L/\delta} \approx e^{-L/\delta}. \quad (3)$$

In these formulas P is the polarization of the beam after passing through the sample, P_0 is the polarization of the incident beam, and g is the gyromagnetic ratio for the neutron.

The dependence of the depolarization on the neutron wavelength was used by us to study the magnetic state of a sample with the aid of neutrons of three different wavelengths ($\lambda_1 = 3.2$, $\lambda_2 = 4.0$, and $\lambda_3 = 4.8$ Å). It follows from (2) that $\ln(P/P_0) \propto \lambda^n$, where $n = 2$ in the case of randomly oriented domains of small dimensions. A change in the magnetic structure of the sample upsets this relation, and causes a change in the exponent n . The function $n(T)$ was determined from the three $P(T, \lambda)$ curves (Fig. 7), and the abrupt change of this dependence yields the temperature region in which domains are formed in the sample. At a polarization measurement accuracy $\Delta P = \pm 1\%$ and at a crystal energy resolution $\Delta \lambda/\lambda \approx 2\%$, we obtain the value of n with accuracy 10%.

Woitowicz and Rayl,^[14] using the molecular-field approximation, considered theoretically the phase transition of an isotropic ferromagnet in an external magnetic field. In contrast to the transition in zero field, when an ordered state is produced in the spin system, the phase transition in an external field is connected with the change in the type of ordering. The transition temperature $T_t(H)$ separates two magnetization states. At $T > T_t(H)$ the sample is homogeneously magnetized, and the region $T < T_t(H)$ corresponds to a state with inhomogeneous magnetization. At the transition point itself $T = T_t(H)$, the saturation magnetization of the sample in an external field H is equal to H/D , where D is the demagnetizing factor of the sample. At this temperature the magnetization curve $M(T)$ as a sharp kink point.^[15] Woitowicz and Rayl obtained the relation

$$T_t(H) = T_c \left[1 - \frac{1}{3} \left(\frac{H}{M_0 D} \right)^2 \right], \quad (4)$$

where $H < M_0$ and M_0 is the magnetization at $T = 0^\circ K$. This study served as theoretical confirmation of the known experimental method of determining $M_S(T)$ and

T_c . With the aid of formula (4) extrapolated to a zero external field one obtains the value of T_c . The method makes it possible to determine also the critical exponents β , γ , and δ of static similarity theory.

Figure 9 shows the temperature $T_t(0)$ obtained from the results of magnetic measurements (Fig. 6) by the method indicated above. $T_t(0)$ was identified in this method with the Curie point. The value of $T_t(0)$ (within the limits of experimental error) coincides on the depolarization curve of Fig. 7 with the temperature at which the derivative $\partial P/\partial T$ has a maximum.

At the same temperature, an abrupt change is observed in the values of n in the spectral dependence of the depolarization $\ln(P/P_0) \propto \lambda^n$. At the kink point on the $P(t)$ curve, where the derivative $\partial P/\partial T$ is maximal, a change takes place in the mechanism whereby the observed projection of the polarization vector is decreased. Above the kink point, the main mechanism is the rotation of P through relatively large angles. According to Halpern and Holstein, the behavior of the polarization is described in this case by formula (3). Below this point, depolarization is produced by small rotations of P in the field of the random domains. From an examination of the results on Figs. 6, 7, and 9, we can conclude that the temperature at which $\partial P/\partial T$ has a maximum and which is defined in accord by the described method as the Curie point, is in fact the domain-formation temperature $T_d = T_t(0)$ at $H = 0$. The true value of T_c , corresponding to the onset of spontaneous magnetization in the sample, lies above T_d ; on the $P(T)$ curve this is the very start of the drop in polarization.

Similar data are contained in^[16], in which simultaneous measurements were made of the depolarization $P(T, H)$ of a neutron beam passing through a nickel sample, and of the magnetic moment $M(T, H)$ induced in the sample by a field H . It follows from Fig. 1 of^[16] that the kink points of the $M(T)$ curves at different values of H , corresponding to the temperature $T_t(H)$, coincide with the temperature at which the derivative of the polarization with respect to temperature $\partial P/\partial T$ is maximal. This temperature characterizes the transition of the system into an inhomogeneous state in the presence of an external field. With increasing field, the value of $T_t(H)$ shifts towards lower temperatures. Consequently, in a strong field the transition into a state with inhomogeneous magnetization occurs at a lower temperature. This explains the shift of the polarization curves $P(T, H)$ measured in different magnetic fields for neutrons with $\lambda \geq 4$ Å, which are given in^[4] on Fig. 5. If we introduce the temperature $T_t(H)$ at which $\partial P/\partial t$ is maximal, then it has a quadratic dependence on H (Fig. 2 of^[17]):

$$T_t(H) = T_t(0) - \alpha' H^2,$$

where $\alpha' = (2.3 \pm 0.3) \times 10^{-3}$ deg/Oe². This confirms the theoretical relation (4) given in^[14]. It is obvious that the temperature $T_t(H)$ introduced in this manner characterizes the formation of domains in the sample. The maxima of neutron scattering through an angle $\theta = 34'$, corresponding to this temperature and shown in Fig. 1b of^[17], are possibly due to the domain-formation process, and not only to critical fluctuations. Extrapolation of the $H^2(T_t)$ plot to a zero external field in accordance with the kink of the magnetization curve (the kink method of^[15]) probably also yields the temperature $T_t(0)$ of the transition to an inhomogeneous mag-

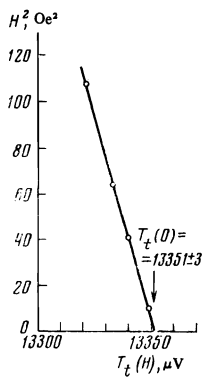


FIG. 9. Determination of the phase-transition temperature from magnetic measurements (Fig. 6) by extrapolation of the $H^2(T_t)$ dependence.

netic phase in a zero field, and not the true value of the Curie temperature.

In our earlier paper on depolarization^[4] we proposed to determine the Curie temperature from the maximum value of the derivative $\partial P/\partial T$ on the $P(T)$ curve. It was assumed that the start of the depolarization in the high-temperature region is connected with the onset of fluctuations of the magnetization, and that the low-temperature part of the depolarization curve was attributed to the onset of a ferromagnetic domain state. The kink point on the depolarization curve, where the derivative $\partial P/\partial T$ is maximal, is the only singular point that joins these two parts of the curve. The same temperature interval included also the observed peak of the small-angle neutron scattering. Without an additional analysis of the result it was impossible to explain in greater detail the physics of the processes observed at that temperature. As follows from the discussed results and from^[9], the onset of macroscopic magnetic order and the domain-formation process can be separated in temperature. Since the main contribution to the depolarization is made by the ferromagnetic phase, the maximum of $\partial P/\partial T$ may not correspond to T_C . Owing to the very narrow $P(T)$ curve, the resultant error in the determination of T_C is less than 0.1° . The large slope of the polarization curve, as shown by the data presented in Figs. 3 and 5, is due to rotation of the polarization vector in the sample. The depolarization observed at this temperature ($P/P_0 = 0.6-0.7$) cannot be attributed to critical fluctuations, as shown by Maleev and Ruban.^[7] Later measurements^[19] of the depolarization of a small-section (0.5 mm^2) neutron beam passing through different points of a nickel sample have shown that at the temperature where $\partial P/\partial T$ is maximal there is produced in the sample an inhomogeneous magnetization. Above this temperature, the beam polarization has identical values in the entire cross section of the sample. These experiments confirm our conclusion that in the immediate vicinity of T_C ($T_d < T \leq T_C$) the sample is in nearly-homogeneous magnetization state. In any case, the dimensions of the regions where the spontaneous magnetization is inhomogeneous are commensurate with the dimensions of the sample.

As to the position of the scattering peak, it follows from Fig. 8 that its maximum lies more readily at the temperature where the depolarization amounts to several per cent (2–3%). Inasmuch as for Ni the temperatures T_d and T_C are close, it is possible that the observed scattering is due both to nuclei of the magnetic phase (“quasidomains”) and to critical fluctuations. It is obvious that phenomena analogous to critical should occur in the temperature region where intense domain

formation takes place. It has not been possible as yet to separate these processes in ferromagnets such as nickel. The half-width of the observed small-angle scattering peak (Fig. 8) is quite large, and the peak overlaps the region of domain formation and T_C . It is possible that it has a finer structure.

Results of a simultaneous measurement of the depolarization of neutrons and absorption of radio frequencies in an yttrium iron garnet were reported in^[19], where the position of the RF absorption maximum was ascribed to critical phenomena. However, the neutron depolarization observed at that temperature ($P/P_0 = 0.5-0.6$) was too high to be able to attribute it to critical fluctuations. It appears that absorption of radio emission is connected also with the domain-formation process.

Thus the improved polarized-neutron procedure offers additional possibilities of analyzing the measurement results and of their physical interpretation. On the basis of the performed measurements it was possible to determine more accurately the temperature of the onset of magnetic order T_C , to establish the domain-formation temperature T_d , and to advance the hypothesis that quasi-homogeneous magnetization exists in the region $T_d < T \leq T_C$. It is obvious that the methods of determining T_C , based on singularities in the behavior of the properties of the magnet (resistivity, the galvanomagnetic effect, radio-emission absorption, etc.) can be connected with domain formation. Knowledge of the exact value of the Curie temperature is important for the determination of the critical exponents of the static similarity theory, as well as for the observation of the region of the influence of the dipole-dipole forces near T_C and for their study.

The authors thank D. M. Kaminker, S. V. Maleev, V. A. Ruban, and A. I. Okorokov for interest in the work and for a discussion of the results, and to V. I. Volkov, Ya. M. Otchik, B. M. Kholkin, and L. A. Shinkevich for help with the experiments.

¹M. K. Savchenko and I. A. Turpanov, *Fiz. Metal. Metalloved.* **33**, 262 (1972).

²L. V. Kirenskiĭ and I. F. Degtyarev, *Zh. Eksp. Teor. Fiz.* **35**, 584 (1958) [*Sov. Phys.-JETP* **8**, 403 (1958)].

³K. P. Belov and Ya. Paches, *Fiz. Metal. Metalloved.* **4**, 28 (1957).

⁴G. M. Drabkin, E. I. Zabidarov, Ya. A. Kasman, and A. I. Okorokov, *Zh. Eksp. Teor. Fiz.* **56**, 478 (1969) [*Sov. Phys.-JETP* **29**, 261 (1969)].

⁵G. M. Drabkin, *Materialy 2-ĭ Mezhdunarodnoĭ shkoly po neĭtronnoĭ fizike v Alushte* (Proc. of 2-nd Internat. School on Neutron Physics in Alushta), Dubna, 1974.

⁶A. I. Okorokov, V. V. Runov, V. I. Volkov, and A. G. Gurasov, *Vektornyi analiz polarizatsii neĭtronov* (Vector Analysis of Neutron Polarization), Preprint No. 106, Leningrad Inst. Nuc. Phys., 1974.

⁷S. V. Maleev and V. A. Ruban, *Zh. Eksp. Teor. Fiz.* **62**, 416 (1972) [*Sov. Phys.-JETP* **35**, 222 (1972)].

⁸Ya. J. Smit and H. Vijn, in: *Ferrity (Ferrites)*, IIL 1962, pp. 323, 252, 261.

⁹G. P. Gordeev, G. M. Drabkin, I. M. Lazebnik, and L. A. Aksel'rod, *Zh. Eksp. Teor. Fiz.* **66**, 1712 (1974) [*Sov. Phys.-JETP* **39**, 841 (1974)].

¹⁰G. S. Kandaurova and Ya. S. Shur, *Fiz. Metal. Metalloved.* **15**, 839 (1963).

- ¹¹G. S. Kandaurova and Ya. S. Shur, *Fiz. Metal. Metalloved.* **16**, 310 (1963).
- ¹²G. M. Drabkin, V. A. Trunov, and A. P. Shchebetov, *Pis'ma Zh. Eksp. Teor. Fiz.* **10**, 527 (1969) [*JETP Lett.* **10**, 336 (1969)].
- ¹³O. Halpern and T. Holstein, *Phys. Rev.* **59**, 960 (1941).
- ¹⁴P. J. Woitowicz and M. Rayl, *Phys. Rev. Lett.* **20**, 1489 (1968).
- ¹⁵A. Arrott, *Phys. Rev. Lett.* **20**, 1029 (1968).
- ¹⁶G. M. Drabkin, E. I. Zabidarov, Ya. A. Kasman, and A. I. Okorokov, *Pis'ma v Zh. Eksp. Teor. Fiz.* **11**, 7 (1970) [*JETP Lett.* **11**, 3 (1970)].
- ¹⁷G. M. Drabkin, A. I. Okorokov, E. I. Zabidarov, and Ya. A. Kasman, *Pis'ma Zh. Eksp. Teor. Fiz.* **8**, 549 (1968) [*JETP Lett.* **8**, 335 (1968)].
- ¹⁸G. M. Drabkin, A. I. Okorokov, V. I. Volkov, and A. F. Shchebetov, *Pis'ma Zh. Eksp. Teor. Fiz.* **13**, 3 (1971) [*JETP Lett.* **13**, 1 (1971)].
- ¹⁹G. M. Drabkin, Ya. A. Kasman, V. V. Runov, I. D. Luzyanin, and E. F. Shender, *Pis'ma Zh. Eksp. Teor. Fiz.* **15**, 379 (1972) [*JETP Lett.* **15**, 267 (1972)].

Translated by J. G. Adashko
193